ELSEVIER

Polymer 42 (2001) 913–923

polymer

www.elsevier.nl/locate/polymer

# The flammability of urethane-modified polyisocyanurates and its relationship to thermal degradation chemistry

C. Dick[a], E. Dominguez-Rosado[a], B. Eling[b], J.J. Liggat[a,*], C.I. Lindsay[c], S.C. Martin[a], M.H. Mohammed[a], G. Seeley[c], C.E. Snape[a]

[a]*Department of Pure and Applied Chemistry, University of Strathclyde, 295 Cathedral Street, Glasgow G1 1XL, UK*
[b]*ICI Polyurethanes (now Huntsman Polyurethanes), Everslaan 45, B-3078 Everberg, Belgium*
[c]*ICI Technology, Wilton Research Centre, Middlesbrough, TS90 8JE, UK*

Received 28 March 2000; accepted 12 June 2000

## Abstract

In this paper we report the use of both in-situ solid-state $^1$H and solid-state $^{13}$C NMR to characterise the condensed-phase residues obtained upon the degradation under inert and oxidative conditions of urethane-modified polyisocyanurate foams based on polypropylene glycol (PPG) and 4,4′-diisocyanato diphenylenemethane (MDI). In particular, we examine the relationship between chain mobility and volatile loss and relate this to the flammability of these materials as characterised by limiting oxygen index (LOI) measurements. Differential scanning calorimetry (DSC), thermogravimetry (TGA) and pyrolysis experiments reveal that the biggest difference in the behaviour of the foams is under inert rather than oxidative conditions. It is thus concluded that the difference in the observed flammability of the samples derives from differences in the volatile release profiles upon degradation in an essentially inert environment. Both DSC and high temperature $^1$H NMR results clearly indicate that there are two major scission processes occurring within the polymers. The lower temperature process is due to the scission of the urethane links, whilst a higher temperature process that becomes increasingly significant as the isocyanurate content of the polymer increases, is due to the scission of the isocyanurate linkages. In addition, $^{13}$C NMR data on the residues clearly show that PPG is lost preferentially from those materials with the highest urethane:isocyanurate ratio. The different fire performance of the four foams under study here is thus ascribed to the conjunction of three factors, all associated with the evolution of PPG or PPG fragments. First, the lower thermal stability of the urethane links leads to facile depolymerisation to yield free PPG from those foams where urethane dominates over isocyanurate linkages. Second, the lower molar mass PPG from these foams is more volatile than that in the isocyanurate dominated foams. Third, the more rigid cross-linked network of the predominately isocyanurate linked foams restricts the diffusion of volatile species formed by and subsequent to the scission of any urethane bonds or the glycol backbone.

*Keywords*: Urethane-modified polyisocyanurates; Flammability; Thermal degradation chemistry

## 1. Introduction

Polymeric materials now play a central role in modern life, but concern about the contribution of these materials to fire deaths [1] remains an obstacle to their still wider use. Many fire retardant additives are available, but whilst effective in reducing gross flammability this is usually achieved at the expense of increased smoke production [2]. Furthermore, these additives, typically based on chlorine, bromine, antimony, zinc or vanadium are increasingly regarded as environmentally unacceptable [3]. Polymers intrinsically capable of producing large quantities of carbonaceous char offer a route to fire retardant systems without these drawbacks. There is a strong correlation between char yield and fire resistance, for not only does char formation occur at the expense of volatile combustible gases but the char also acts as a barrier, sealing the polymer against oxygen ingress and volatile product egress [4]. Whilst the importance of char is appreciated, the chemistry of its formation is largely neglected [5]. Most mechanistic studies of polymer thermal degradation concentrate solely on volatile products [6] with the residue, often highly cross-linked even in the early stages of degradation, simply regarded as ‘intractable’. This principally reflects the limited availability of appropriate means of analysing the residue. However, the advent of increasingly sophisticated solid-state NMR techniques provides the opportunity for the direct and detailed characterisation of condensed-phase chemistry, in char-forming polymers such as the polyurethanes.

Whilst solid-state $^{13}$C NMR is well-established as a

---

* Corresponding author. Tel.: + 44-141-548-4351; fax: +44-141-548-4822.

*E-mail address:* j.j.liggat@strath.ac.uk (J.J. Liggat).

0032-3861/01/$ - see front matter
PII: S0032-3861(00)00470-5

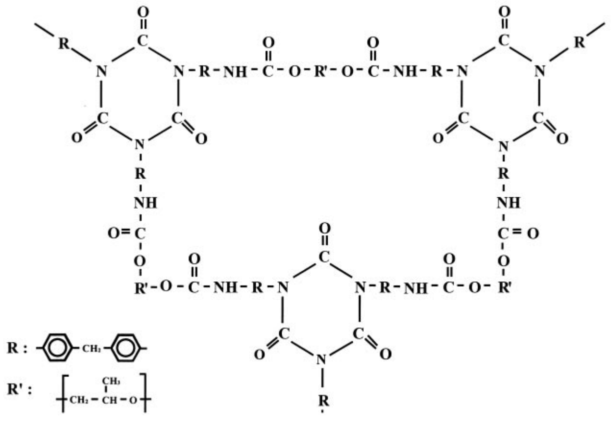

Fig. 1. Structure of urethane-modified polyisocyanurates.

technique for the structural elucidation of polymers, broadline $^1$H NMR, which has a long history in the investigation of the mobility of coals and pitches during their carbonisation [7–9], is much less frequently encountered in polymer science. Indeed, its use in polymer thermal degradation studies has only recently been reported [10]. In polymers there are usually two contributions to the free induction decay (FID), one from a mobile and one from a rigid component. The former displays Lorentzian decay and the latter, Gaussian. The peak width of the spectrum is inversely proportional to the $T_2$ (the spin–spin relaxation time) of the fluid phase. Both are highly responsive to changes in mobility and this can be investigated as a function of temperature. In this paper we report the use of both in-situ solid-state $^1$H and solid-state $^{13}$C NMR to characterise the condensed phase of urethane-modified polyisocyanurate foams based on polypropylene glycol (PPG) and 4,4′-diisocyanato diphenylenemethane (MDI). In particular, we examine the relationship between chain mobility and volatile loss and relate this to the polymer structure.

Urethane-modified polyisocyanurates such as those studied here (Fig. 1) are widely used in public and domestic buildings. Indeed, their use as construction materials is increasing steadily because of their superior insulation properties and easy processability. Concern about the flammability of foamed materials has led to the enactment of strict building regulations, which has provided some constraint on the continuing growth of their use, although it is recognised that isocyanurate-based foams possess better heat and flame resistance than simple polyurethanes.

The isocyanate–polyol stoichiometry [11] plays an important part in determining the structure and thermal properties of urethane-modified polyisocyanurates as it controls the relative amounts of urethane and isocyanurate linkages. An important characteristic is the amount of isocyanate used, commonly expressed as the isocyanate index (a measure of the amount of isocyanate used relative to the theoretical stoichiometric amount). As a result of the considerable excess of isocyanate, very high index foams have a large proportion of the trimeric cyclic isocyanurate structures that impart resistance and thermal stability to the polymer. The isocyanurate linkage has an inherently higher thermal stability than that of the urethane linkage (the latter dissociates easily at about 200°C) [12], and it has been found that in general flammability decreases as the proportion of isocyanurate in the foam increases [13–16]. For example, Cunningham et al. [16] undertook a study on the flame resistance of a series of polyisocyanurates similar to those studied here. They found that at a fixed isocyanate mass fraction the limiting oxygen index (LOI) increases with the increasing molecular mass of the polypropylene glycol (PPG) used in the formulation. Over a range of isocyanate mass fractions, they found the LOI of foam based on PPG of molecular mass 200 to be consistently lower than that of a foam based on PPG of molar mass 425. The difference was most pronounced at isocyanate mass fractions above 0.6, where the difference in LOI was of the order of three percentage points. The LOI values for foams prepared from polypropylene glycols of molar mass 1000 and 2000 were indistinguishable from one another even though their isocyanate indices varied by a factor of two, but were consistently about one percentage point higher than the PPG-425 materials. The authors ascribed the pronounced differences between PPG-200 based foams and the others, particularly at higher isocyanate mass fractions, to the onset of the formation of the considerably more stable isocyanurate links in the PPG-425, PPG-1000 and PPG-2000 as a result of the higher isocyanate index of these latter formulations. The authors also noted that at isocyanate indices above 600, and for polypropylene glycols of molecular mass 425 and above, the LOIs were dependent on only the mass fraction of isocyanate, hence explaining the identical behaviour of the PPG-1000 and PPG-2000 foams.

In order to relate the observed fire behaviour with the degradation of these materials on a molecular basis, Gao et al. [17] studied by laser-pyrolysis time of flight mass spectrometry a similar series of foams based on PPG-425. They found that as the isocyanate index of the foams increased, the yield of polyol (the major volatile product) decreased whilst the yield of $CO_2$ (found to be a product of the decomposition of isocyanurate) increased. These workers thus ascribed the increase in LOI with isocyanate index to a reduction in the production of flammable polyol. The observation by Gao et al. that polyol was the major degradation product is consistent with the known degradation behaviour of urethane-based polymers.

Although the formulation of urethane-derived polymers is complex, the key features of the degradation chemistry have been identified. The degradation mechanisms of simple polyurethanes derived from poly(ethylene glycol) (PEG) and 4,4′-diisocyanato diphenylenemethane (MDI) were studied in detail by Grassie and co-workers [18,19]. Under inert conditions, at temperatures above about 210°C the polyurethane linkage disappears without any volatile

Table 1
Compositional and limiting oxygen index data for the four foams

| Polymer | Foam 1 | Foam 2 | Foam 3 | Foam 4 |
|---|---|---|---|---|
| Polyol | PPG-200 | PPG-425 | PPG-1000 | PPG-2000 |
| Polyol content (phr) | 25 | 25 | 25 | 25 |
| Isocyanate content (phr) | 75 | 75 | 75 | 75 |
| Blowing agent (F141b) content (phr) | 16 | 16 | 16 | 16 |
| Isocyanate index | 219 | 460 | 1066 | 2078 |
| Limiting oxygen index | 20.4 | 21.2 | 21.8 | 22.0 |

products being formed, and the initial degradation step is seemingly a simple depolymerisation reaction. The two monomers are the primary products and all the other products, which include carbon dioxide, butadiene, tetrahydrofuran, dihydrofuran and water as volatile products and carbodiimide and urea amide in the condensed phase, are formed from the monomers in a complex cascade of secondary reactions while they are diffusing from the hot polymer. This proposal has been confirmed by Ravey and Pearce [20], Herzog [21] and Jeffs [22]. Under oxidative conditions, Gaboriaud and Vantelon [23] found that the first step involves the scission of the polyurethane molecule into primary amine, carbon dioxide and propenyl ether species, the latter leading to propene formation. The mechanism was reduced to a depolymerisation process followed by radical breakdown of the polyol chain in conjunction with simple radical formation. The radicals formed can explain the formation of various gaseous species during the heating programme.

## 2. Experimental

### 2.1. Materials

ICI Polyurethanes, Everberg, Belgium, supplied four rigid polyurethane–isocyanurate (PIR) foams (PIR1-4) based on 4,4′-diisocyanato diphenylenemethane (MDI) and polypropylene glycol (PPG) with average molecular masses of 200, 425, 1000 and 2000 (PPG-200, PPG-425, PPG-1000 and PPG-2000, respectively). These were similar in formulation to the materials studied previously [13,16]. A brief summary of the composition is given in Table 1.

### 2.2. Limiting oxygen index (LOI)

Tests were carried out at the ICI Technology Centre, Wilton, UK. The test was conducted according to the standard procedure ASTM D2863-91. A mixture of oxygen and nitrogen of known composition is metered into the bottom of a tube passing through a bed of glass beads 3–5 mm in diameter and 80–100 mm deep to smooth the flow of the glass. The foam is ignited at its upper end with a flame, which is then withdrawn, and the atmosphere that just permits steady burning down the sample is determined. Six strips with dimensions of $1.2 \times 1.2 \times 10$ cm were prepared from each foam. Results are summarised in Table 1 for the four foams investigated.

### 2.3. Pyrolysis

The foams were pyrolysed in a fixed bed reactor of Incoloy construction, which has been described previously [24]. To program the resistive heating from 250 to 550°C with a heating rate of 10°C $\text{min}^{-1}$, a Eurotherm model 818 controller was used. The isothermal dwell time for all the temperatures was 20 min. The sweep gas used was nitrogen with a flow of 0.3 $\text{dm}^3\,\text{min}^{-1}$. The tars were collected in a trap cooled with dry ice, and after each run were recovered in dichloromethane for analysis. All chars were ground in a mortar to $< 212$ μm. Char yields were calculated from direct weighing of the char recovered. Tar yields were determined from the weight gain of the trap.

To obtain chars from foams based on PPG-200 and PPG-2000 (foams 1 and 4) under air, 0.5 g of the foam was processed with the same conditions as above and with flows of 0.3 and 1.0 $\text{dm}^3\,\text{min}^{-1}$. However, under these conditions, the foams self-ignited, and to obtain chars for analysis, 0.5 g of foam was placed in an open crucible and heated in a furnace from ambient to temperatures in the range of 250–550°C with a hold time of 1 h.

### 2.4. Microanalysis

C, H and N contents of the chars were determined using a Perkin Elmer Series II Analyser 2400.

### 2.5. Differential scanning calorimetry (DSC)

DSC measurements were carried out using a Du Pont model 9900 instrument, which was calibrated with indium. Before starting any run, the oven was cleaned by heating it to 400°C and holding for 15 min. A sample weight of about 6 mg was compacted into an aluminium pan so as to provide good thermal contact with the sample vessel and to optimise the heat flow between the heat source and the sample. Pans were sealed and the lids pierced so that the sweep gas contacts the sample. All analyses were conducted under nitrogen or air at a flow rate of 80 ml $\text{min}^{-1}$, with a heating rate of 10°C $\text{min}^{-1}$ from 50 to 550°C.

### 2.6. Thermogravimetric analysis

A Stanton Redcroft TG-750 thermogravimetric analyser was used. The instrument was calibrated following the manufacturer's recommended procedures. About 0.4–0.6 mg of foam was used to obtain the TG profiles. The sample was placed in a holder and introduced into a micro-furnace, which is cooled with water. The heating rate was at 10°C $\text{min}^{-1}$ under a flow of 10 ml $\text{min}^{-1}$ of nitrogen or air. The results were plotted as weight loss versus potential. By means of tables, the potential (millivolts) reading was converted into temperature (°C), to plot the percent weight loss versus temperature.

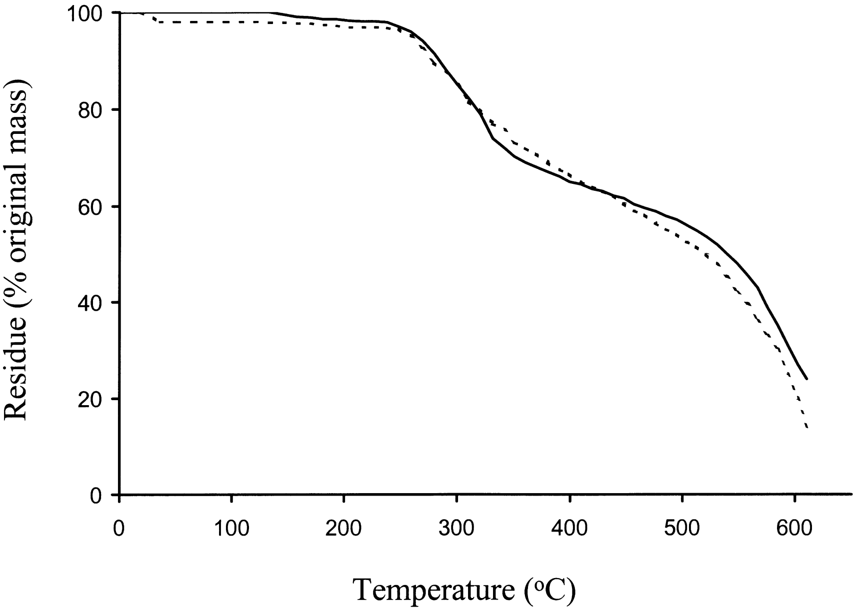

Fig. 2. Thermogravimetry curves for foams 1 (—) and 4 (-); degradation under air.

### 2.7. Fourier transform infrared spectroscopy

Infrared spectra of the tars and chars were obtained using a Mattson 5000 and a Nicolet Impact 400D FTIR instrument, respectively.

### 2.8. Solid-state NMR

#### 2.8.1. High temperature in-situ $^1H$ NMR

In the 100 MHz Doty NMR probe used, the 90° pulse width varied with temperature between 2.2 μs at ambient to 3.0 μs at 600°C. The temperature of the sample was monitored by two thermocouples simultaneously; one of these was touching the container of the sample, and the other was close to the heater. The system was calibrated using compounds of known melting point (phenanthrene, 100°C; methyl red-2-[4-(dimethylamino) phenyl-azo] benzoic acid 179°C; 2,2′-dithiodibenzoic (salicylic) acid, 288°C and decacylene, 395°C). The solid echo pulse sequence (90°–$\tau$–90°) with a refocusing of 5 μs is used in order to minimise the loss of signal due to the dead time of the NMR coil.

Approximately 50 mg of finely powdered foam was packed into the zirconia container, which is placed horizontally in a stator. A flow of 12 $\mathrm{dm^3\,min^{-1}}$ of dry nitrogen was used to transfer heat to the samples and to remove the volatiles that escape through a small ventilation hole in the container. Spectra were obtained at a number of different temperatures using the solid echo pulse sequence. 256 scans were accumulated with the recycle delays being between 300 ms and 1 s. The time-domain decays of the solid echo signals were transferred from the spectrometer to computer (Power Mac 6000). The FIDs were processed using the Bruker program WinNMR 3.1. The results are saved in ASCII code, which allows files to be opened in Microsoft Excel. The files were numerically analysed using a macro program SIMFIT (created in the laboratory by PhD students) in Microsoft Excel version 4.0. This program, by numerical calculation, allows the fitting of Lorentzian and Gaussian components to the original spectra. The proportions of Lorentzian and Gaussian components in the samples at each temperature were also checked by cutting and weighing the peaks and were found, within experimental error (±2–3% of the total hydrogen), to be in close agreement with the proportions obtained from the fitting program.

#### 2.8.2. Solid-state $^{13}C$ NMR

The $^{13}$C NMR measurements were carried out on a Bruker MSL 100 spectrometer, operating at 25 MHz with magic angle spinning (MAS) at 5 kHz to give spectra in which the total intensities are only ca. 6% of the central aromatic bands for aromatic carbons. The $^1$H decoupling and spin-lock fields are ca. 60 kHz. Tetrakis (trimethylsilyl)-silane (TKS) was used as an internal standard. The spectra were accumulated using the cross polarisation (CP) technique. Contact times applied were 1 and 5 ms. A recycle delay of 2 s and 3000 scans were used for the analysis. The areas of the aromatic and aliphatic peaks were measured by using both electronic integrals and cutting and weighing the peaks.

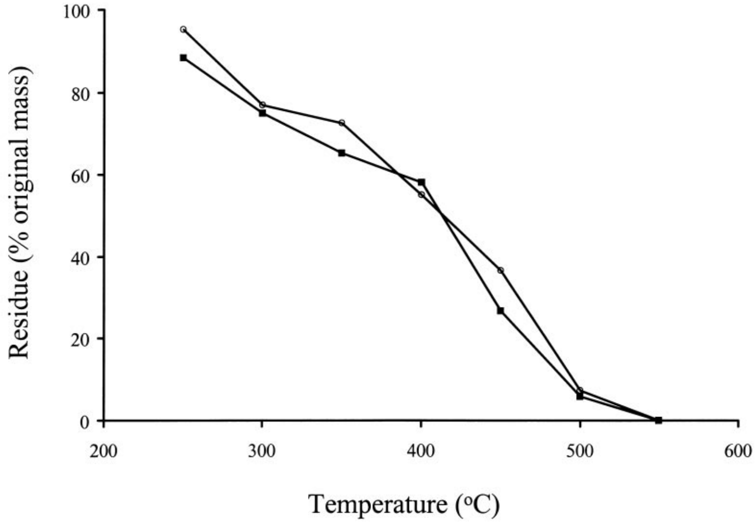

Fig. 3. Residue as a function of isothermal degradation temperature for foams 1 (■) and 4 (○) pyrolysed under air.

## 3. Results and discussion

### *3.1. Limiting oxygen index and degradation under air*

The LOI values of the four samples are recorded in Table 1. The values show that sample 1 is considerably more flammable than samples 2–4. Of course, a longstanding debate amongst polymer flammability and degradation experts is on the relevance of inert atmosphere degradation studies to flammability issues. Whilst the combustion process itself must occur de facto under oxidative conditions, the limited diffusion of oxygen into polymers combined with oxygen depletion at the flame front requires that the initial degradation in the polymer-condensed phase must be primarily non-oxidative. Of course, in thin-walled open-celled foams such as those investigated here, one may expect oxidation to play a rather more important role than in, for example, a moulded slab of polyester resin. Here, however, the degradation experiments under air do not themselves seem able to account for the differences observed in the LOI tests. Indeed, both foams 1 and 4 have very similar TGA behaviour under air (Fig. 2), and at higher temperatures foam 4 is marginally less stable than foam 1. Interestingly, both samples show something of a plateau of stability between 350 and 500°C. The results from the open crucible pyrolyses in air mirror closely the TGA experiments (Fig. 3). Although the stable plateau is not apparent, it is clear that the degradation is essentially

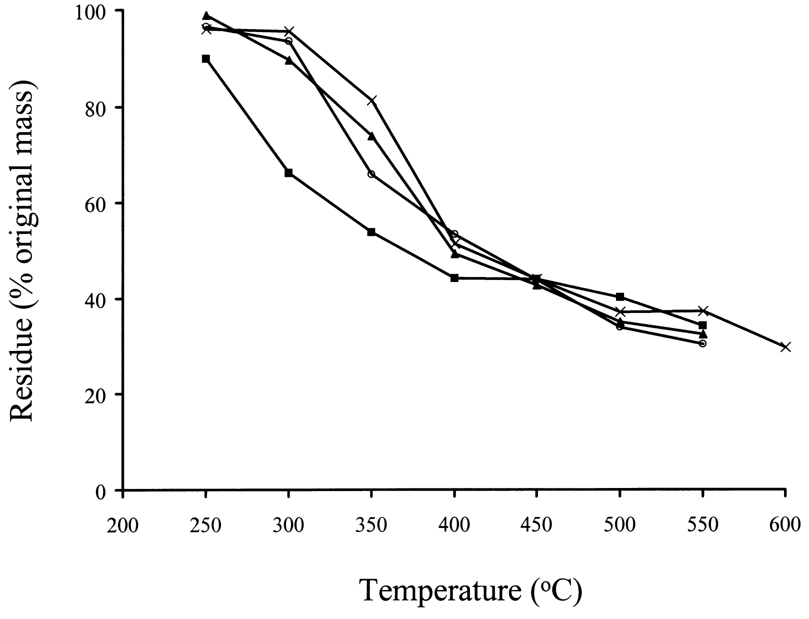

Fig. 4. Residue as a function of isothermal degradation temperature for samples pyrolysed under nitrogen. (■, Foam 1; ▲, foam 2; ×, foam 3; ○, foam 4.)

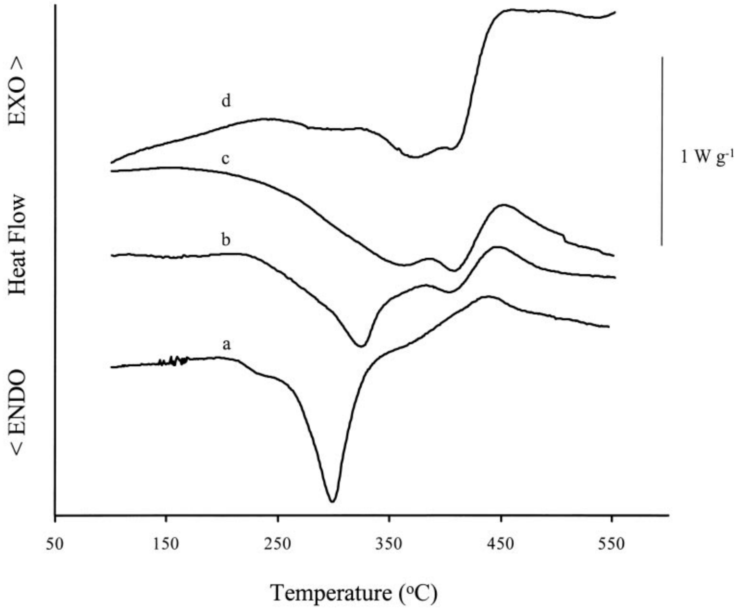

Fig. 5. Comparison of DSC behaviour under nitrogen for foam 1(a), foam 2(b), foam 3(c) and foam 4(d). Curves are on the same scale but have been offset for clarity.

occurring in two steps. As with the TGA experiments these pyrolyses show foam 4 to be marginally more stable around 350°C and less stable at 450°C, although the difference is just on the margin of experimental error (±5 percentage points).

### 3.2. Degradation under nitrogen

Whilst degradation under air shows the degradation profiles of foams 1 and 4 to be similar, there are marked differences in the behaviour under nitrogen, which seemingly reflect the differences in LOI. For example, the profiles for the mass loss as a function of temperature (Fig. 4) show foam 1 to be markedly less stable between 250 and 400°C than the other foams. Similarly, the DSC curves for the four foams heated under nitrogen (Fig. 5) show foam 1 to be less stable than the others. A low temperature degradation process peaking around 315°C (foam 1) becomes progressively less important as the molar mass of the polyol component is increased whilst a higher temperature process becomes increasingly dominant. Thermogravimetric analysis was undertaken on the two foams of extreme composition, foams 1 and 4 (Fig. 6). Again, foam 1 is shown to be markedly less stable than foam 4. Whilst the ultimate residual mass is higher than for the furnace pyrolysis, it must be remembered that the latter samples, although also heated at 10°C min$^{-1}$, were subsequently held isothermally at the degradation temperature for 20 min. However, it is interesting to observe that under TGA conditions the residue at 550°C for foams 1 and 4, respectively is 38 and 48%, whilst under furnace pyrolysis conditions, the residues at 550°C were 34 and 30%, respectively. The DSC and TGA curves for foam 1 (predominantly urethane linked) closely resemble those obtained by Grassie and Mendoza [19] for a polyurethane derived from MDI and PEG of molecular mass 200. In that system, the authors identified the onset of degradation with the depolymerisation of the urethane bonds to produce the starting monomers. Under atmospheric pressures, the monomers volatilise only slowly from the condensed phase and undergo a series of further reactions, some of them scissions that produce more volatile chain fragments and rearrangement products (typically, for example, acetaldehyde from the PEG sequences), and some of them cross-linking reactions (for example, the reaction of urethane structures with carbodiimide formed by the dimerisation of newly formed isocyanates). Whilst of course in our polymers the polyol is PPG rather than PEG, the

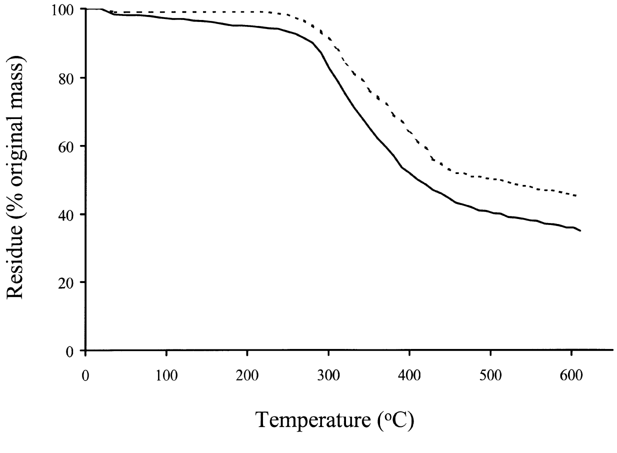

Fig. 6. Thermogravimetry curves for foams 1 (—) and 4 (-); degradation under nitrogen.

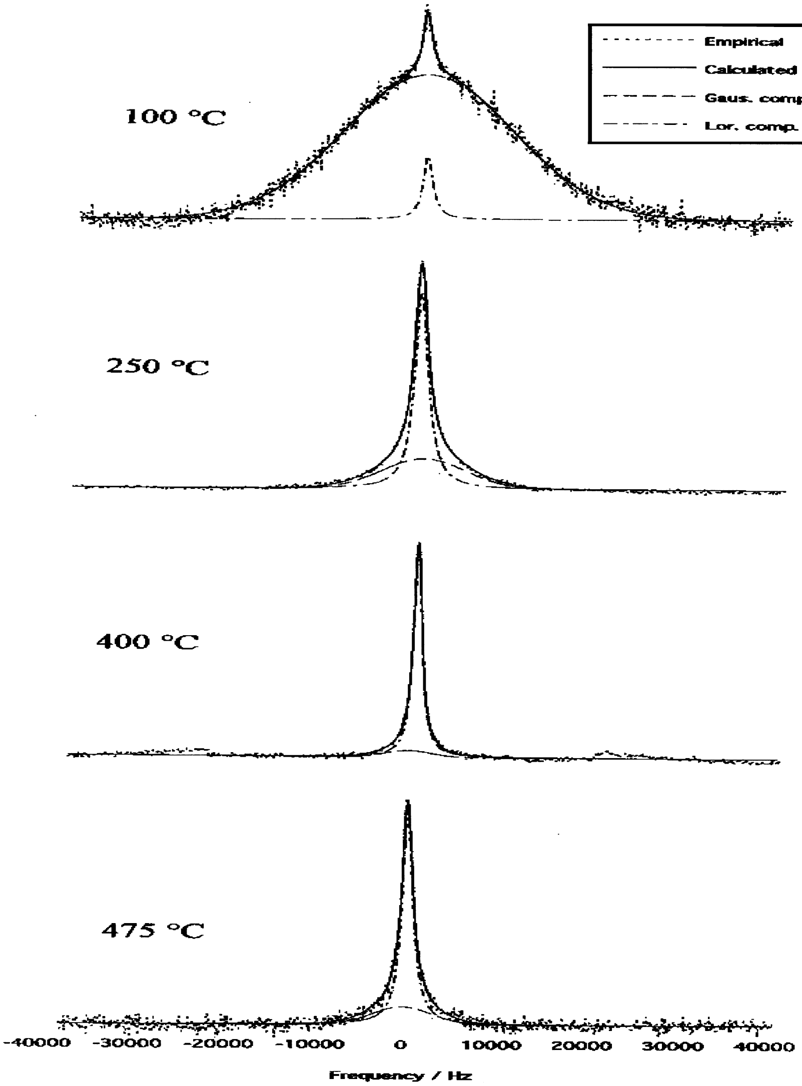

Fig. 7. High temperature in situ $^1$H NMR spectra of foam 1.

urethane scission process should be essentially unchanged, and the degradation of PPG follows the same pattern as PEG [25,26]. The major degradation products from PPG, acetaldehyde and propionaldehyde, are particularly problematic in terms of overall flammability, as their auto-ignition temperatures are very low [27].

### 3.3. Solid-state $^1$H NMR

The variable temperature solid-state $^1$H NMR experiments provide an insight into the physical changes occurring upon degradation in an inert atmosphere (Figs. 7–9). At 100°C, foam 4 has a much higher Lorentzian (mobile) component than foam 1. This is consistent with the polymer structures, as although foam 4 is more highly cross-linked via isocyanurate structures, the much longer polyol component is less constrained by the aromatic hard blocks than is the case in foam 1. Upon heating, as one would expect, there is an increase in mobility, evident for both foams between 100 and 250°C. Foam 1 shows, however, much the larger *increase* in the mobile component. This is indicative of high levels of chain scission (associated with the cleavage of the urethane bonds) with a commensurate increase in polyol mobility as the constraints on motion are reduced. In contrast, significant chain scission does not occur in foam 4 until the cleavage of the isocyanurate links above 300°C, and as a consequence the *increase* in mobility is much less. Both foams show increased mobility as the temperature is increased further, and by 400°C foam 1 is essentially fully fluid. In contrast foam 4 approaches full fluidity at 475°C. Indeed, consideration of the Gaussian spin–spin relaxation time, $T_2$(g), a direct measure of the fluidity of the Gaussian component, for both polymers over the range 250–450°C shows that the rigid component of foam 4 is much less mobile than that of foam 1, which is consistent

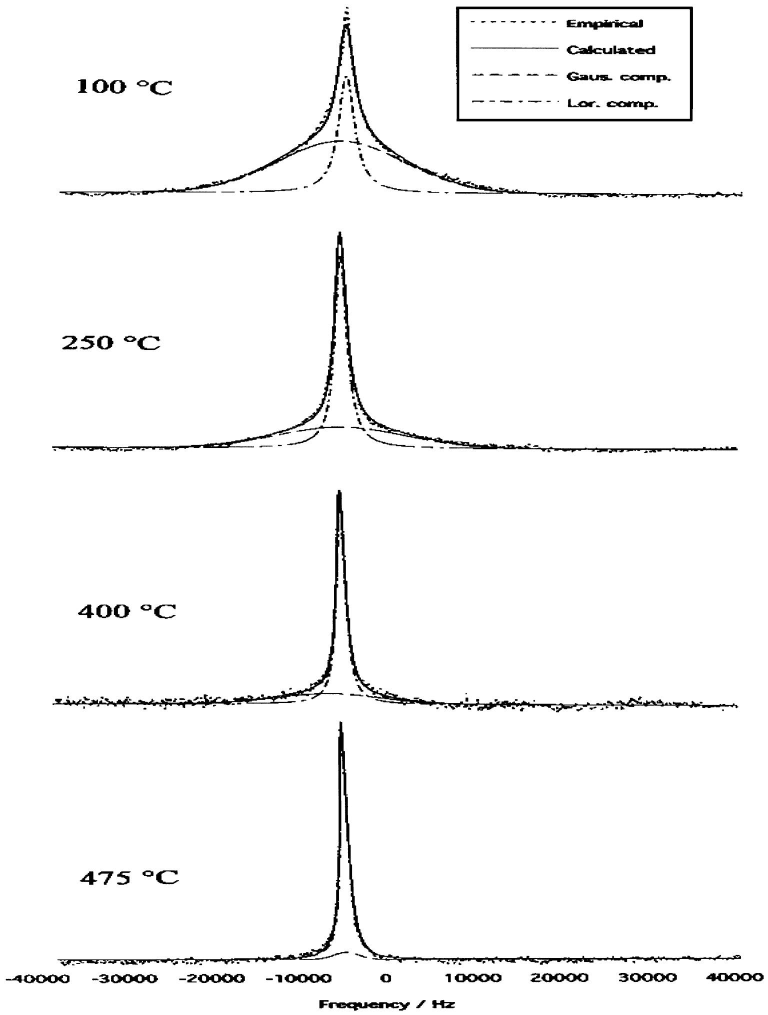

Fig. 8. High temperature in situ $^1$H NMR spectra of foam 4.

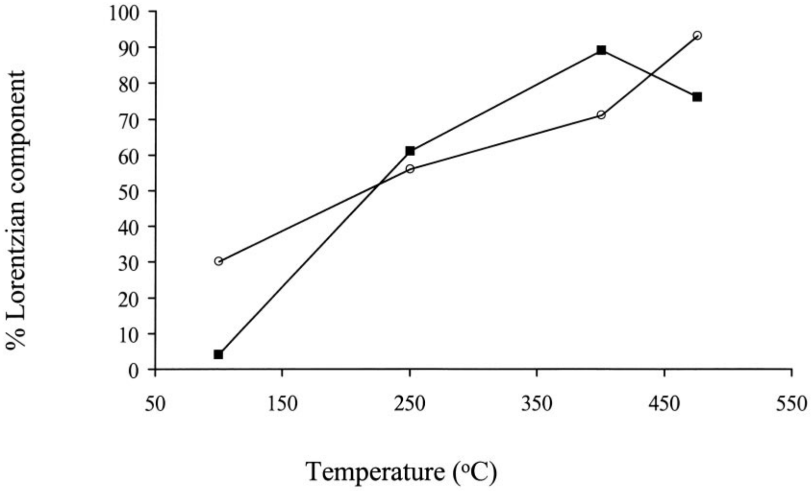

Fig. 9. Lorentzian (mobile) component of broad band $^1$H spectra as a function of temperature for foams 1(■) and 4 (○).

Table 2
Spin–spin relaxation time, $T_2$(g), for the Gaussian component as a function of temperature. ( * — at 450°C, foam 1 is completely fluid)

| Temperature (°C) | Foam 1 | Foam 4 |
|---|---|---|
| 250 | 48 | 30 |
| 400 | 87 | 37 |
| 450 | * | 67 |

with the expected cross-linking role of the isocyanurate functionality (Table 2).

### 3.4. Solid-state $^{13}$C NMR

Solid-state $^{13}$C NMR spectra of the residues obtained from the furnace pyrolyses under nitrogen provide structural information on the condensed-phase chemistry. Figs. 10 and 11 show CP-MAS spectra for undegraded foams 1 and 4, and for the residues obtained upon pyrolysis to 250, 300 and 350°C. Looking initially at the undegraded polymers, the peak at 20 ppm represents the methyl of polyol, the 45 ppm peak corresponds to the ring bridging methylene of MDI, peaks between 70 and 80 ppm are due to the polyol methylene, and the aromatic envelope (including the isocyanate derived C=O) lies between 100 and 160 ppm. From these spectra and microanalysis data, we can derive the carbon distribution of the foams and residues. Fig. 12 shows the aromatic and polyol content as a function of temperature, normalised to the initial content in the undegraded foams. As the temperature is increased, the polyol content decreases; this loss being more rapid for foam 1. Although the aromatic content of foam 1 is slightly lower than foam 4 (74 to 78%) this alone does not seem sufficient to account for the faster polyol loss. For both foams, the loss of aromatic carbon is small compared to the polyol loss. Again, foam 4 is shown to be markedly more stable than foam 1.

## 4. Conclusions

Clearly, the DSC, TGA and pyrolysis experiments reveal that the bigger difference in the behaviour of the foams is

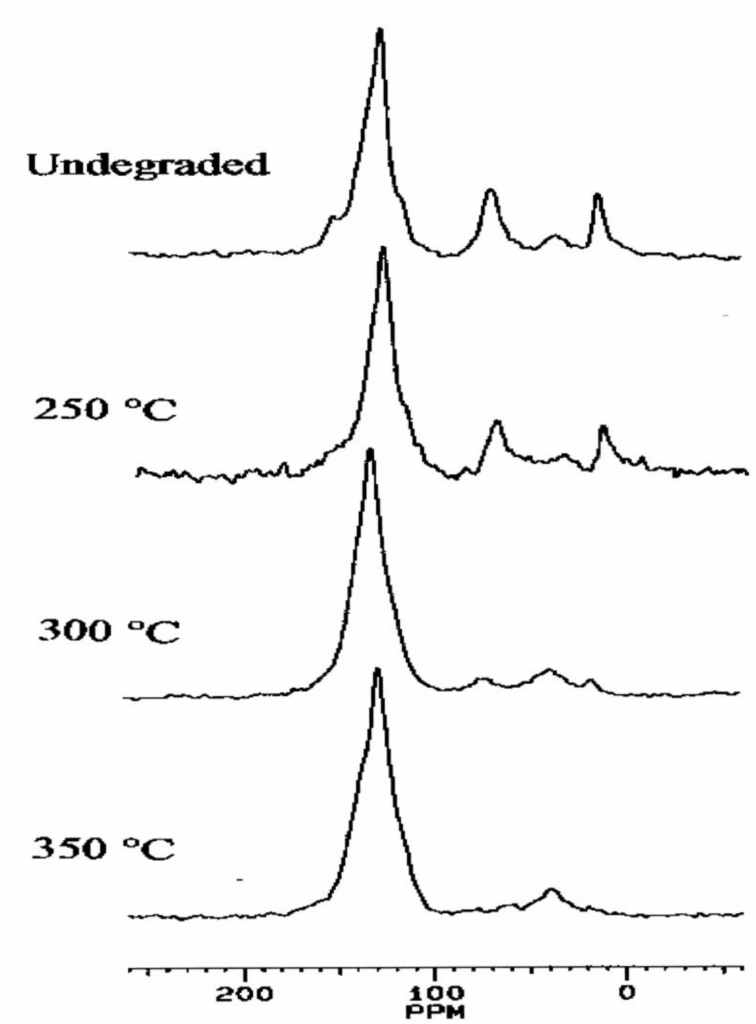

Fig. 10. $^{13}$C NMR spectra of residues obtained from foam 1 after pyrolysis in nitrogen.

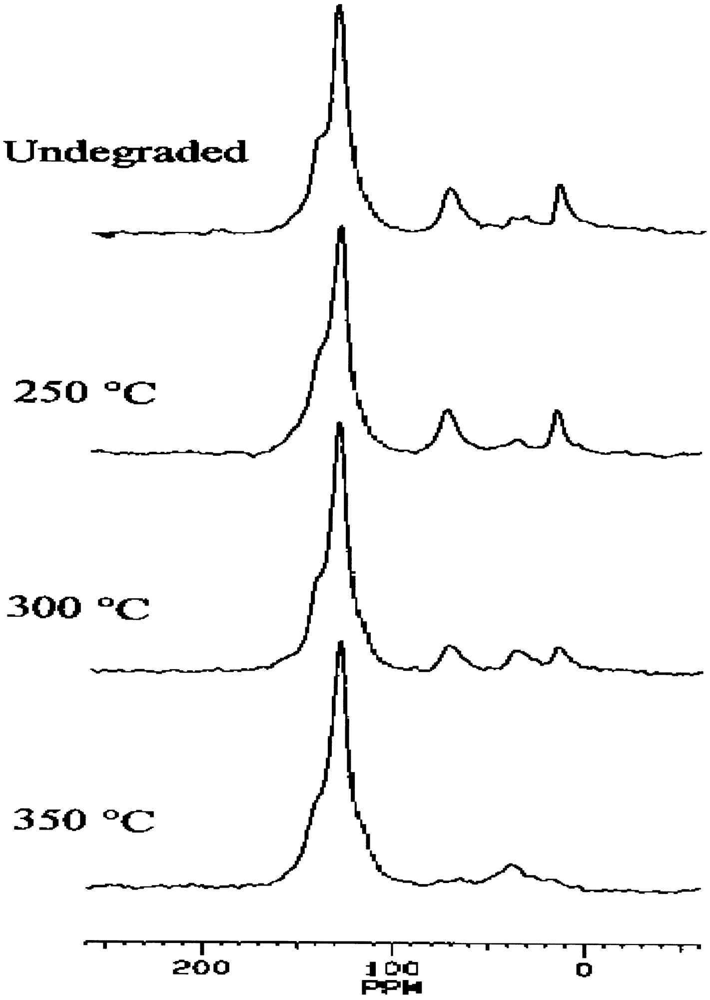

Fig. 11. $^{13}$C NMR spectra of residues obtained from foam 4 after pyrolysis in nitrogen.

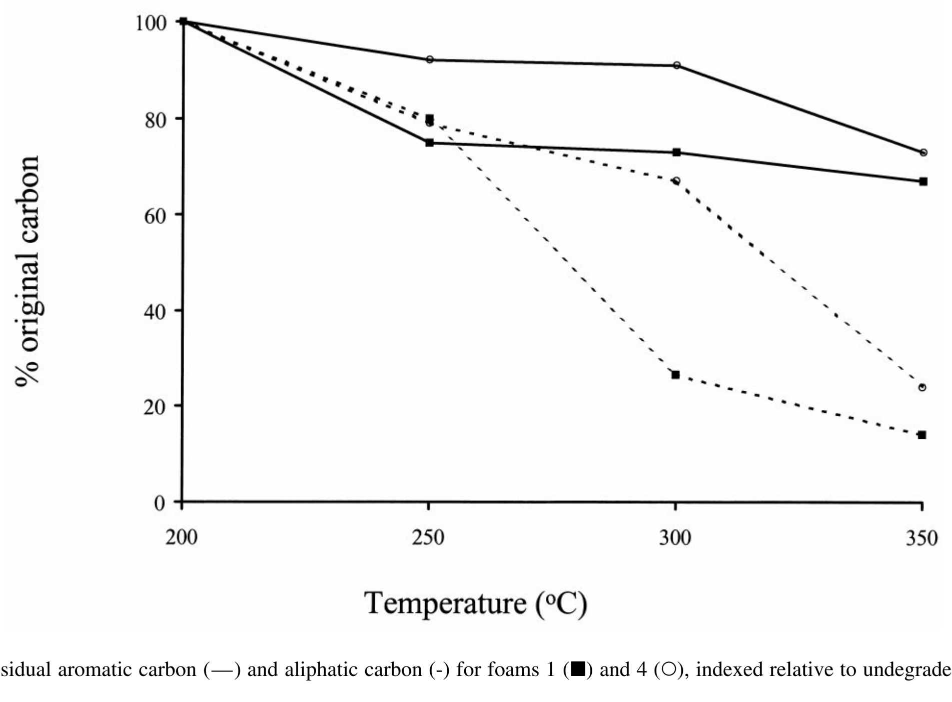

Fig. 12. Residual aromatic carbon (—) and aliphatic carbon (-) for foams 1 (■) and 4 (○), indexed relative to undegraded material.

under inert rather than oxidative conditions. It is thus tempting to conclude that the difference in the observed flammability of the samples derives from differences in the volatile release profiles upon degradation in an essentially inert environment. The DSC clearly indicates that there are two major scission processes occurring within the polymers. The lower temperature process, dominant in the largely urethane-linked polymer (foam 1), can be ascribed to the scission of the urethane links, whilst the higher temperature process, which becomes increasingly significant as the isocyanurate content increases, is due to the scission of the isocyanurate linkages. The observed degradation temperatures are consistent with those reported in the literature [12,18,19].

High temperature $^{1}$H NMR clearly shows the changes in mobility associated with chain scission, and the mobility-reducing influence of the isocyanurate groups. In addition, as the $^{13}$C NMR data on the residues clearly show (Figs. 10 and 11), polyol is lost from foam 1 at much lower temperatures than foam 4. The different fire performance of the four foams under study here can be ascribed to the conjunction of three factors. First, the lower thermal stability of the urethane links leads to the release at lower temperature of polyol from those foams where urethane dominates over isocyanurate linkages (i.e. the PPG-200 and PPG-425 systems). Second, as the molecular mass of the polyol increases, more scissions are required per molecule to produce fragments small enough to volatilise from the system. Third, the more rigid cross-linked network of the predominately isocyanurate linked foams (i.e. the PPG-1000 and PPG-2000 systems) restricts the diffusion of volatile species formed by and subsequent to the scission of any urethane bonds or the glycol backbone. The increased rigidity in the presence of the isocyanurate groups is clearly shown in the high temperature $^{1}$H NMR spectra where the mobility of foam 1 increases above 200°C (as the urethane bonds breaks) whilst the mobility of foam 4 increases only above 300°C (the degradation temperature of the isocyanate units). The $^{13}$C NMR results are also consistent with this interpretation and show clearly the greater retention of both the aromatic and polyol component in foam 4 at temperatures below 300°C. Above 300°C and the cleavage of the isocyanurate structures, the loss profile of foam 4 starts to approach that of foam 1. The furnace pyrolyses also show that the onset of degradation progressively increases as the isocyanate content increases. That the mass loss profiles of foams 2–4 are similar and markedly different from foam 1 is in line with previous work, where it was concluded that for foam systems of relatively high mass fractions of isocyanate, the isocyanate index (and by implication in this case polyol molar mass) is not a major determinant of the LOI value. This may be because there exists a critical threshold of isocyanurate units sufficient to hinder the volatilisation of low molecular mass species. Overall, therefore, we argue that the improvement in flame resistance, as measured by the LOI test, is due to reduced volatile loss in the isocyanurate-rich foams.

## References

[1] Morikawa T, Yanai E, Okada T, Watanabe T, Saito Y. Fire Safety J 1993;20:257.

[2] Starns Jr. WH, Edelson D. Macromolecules 1979;12:797.

[3] Lomakin SM, Zaikov GE, Artiss MI. Int J Polym Mater 1996;32:173.

[4] Cullis CF, Hirschler MM. The combustion of organic polymers. Clarendon Press, 1981.

[5] Carty P, White S. Polymer 1994;35:343.

[6] Grassie N, Scott G. Polymer degradation and stabilisation. Cambridge University Press, 1984.

[7] Miyazawa K, Yokono T, Sanada Y. Carbon 1979;17:223.

[8] Maroto-Valer MM, Andresen JM, Snape CE. Fuel 1997;76:1301.

[9] Maroto-Valer MM, Andresen JM, Snape CE. Energy Fuels 1997;11:236.

[10] Dick C, Liggat JJ, Snape CE. Oral presentation to the Polymer Degradation Discussion Group, Salford, September 1998.

[11] Wood G, editor. The ICI polyurethanes book 2. Chichester: ICI/Wiley, 1990.

[12] Duff DW, Maciel GE. Macromolecules 1991;24:651.

[13] Reymore HE, Lockwood RJ, Ulrich H. J Cell Plast 1979;14:332.

[14] Nawata T, Kresta JE, Frisch KC. J Cell Plast 1975;11:267.

[15] Imai Y, Inukai T, Tamashima M. J Fire Sci 1983;1:348.

[16] Cunningham A, Eling B, Sparrow DJ. Cell Polym 1987;6:42.

[17] Gao F, Price D, Milnes GJ, Eling B, Lindsay CI, McGrail PT. J Anal Appl Pyrol 1997;40–41:217.

[18] Grassie N, Zulfiqar M. J Polym Sci, Polym Chem Ed 1978;16:1563.

[19] Grassie N, Perdomo Mendoza GA. Polym Degrad Stab 1985;10:267.

[20] Ravey M, Pearce EM. J Appl Polym Sci 1997;63:47.

[21] Herzog K. Makromol Chem, Macromol Symp 1991;52:307.

[22] Jeffs GM, Sand H. Cell Polym 1984;3:401.

[23] Gaboriaud F, Vantelon JP, Breillat C. J Polym Sci, Polym Chem 1982;20:2063.

[24] Rocha JD, Brown SD, Love GD, Snape CE. J Anal Appl Pyrol 1997;40–41:91.

[25] Costa L, Camino G, Luda MP, Cameron GG, Qureshi MY. Polym Degrad Stab 1995;48:325.

[26] Costa L, Camino G, Luda MP, Cameron GG, Qureshi MY. Polym Degrad Stab 1996;53:301.

[27] Lewis RJ, editor. Sax's dangerous properties of industrial materials 8. New York: Van Nostrand Reinhold, 1992.